A Comparative Study of Computational Solutions to Flow Over a Backward-Facing Step

M. Mizukami, N.J. Georgiadis, and M.R. Cannon
Lewis Research Center
Cleveland, Ohio

Reprint from, "Fifth Annual Thermal and Fluids Analysis Workshop,"
a conference held at
NASA Lewis Research Center, Cleveland, Ohio
August 16–20, 1993

NASA

A COMPARATIVE STUDY OF COMPUTATIONAL SOLUTIONS TO FLOW OVER A BACKWARD-FACING STEP

M. Mizukami, N. J. Georgiadis and M. R. Cannon
National Aeronautics and Space Administration
Lewis Research Center
Cleveland, Ohio 44135

SUMMARY

A comparative study was conducted for computational fluid dynamic solutions to flow over a backward-facing step. This flow is a benchmark problem, with a simple geometry, but involves complicated flow physics such as free shear layers, reattaching flow, recirculation, and high turbulence intensities. Three Reynolds-averaged Navier-Stokes flow solvers with k-ε turbulence models were used, each using a different solution algorithm: finite difference, finite element, and hybrid finite element - finite difference. Comparisons were made with existing experimental data. Results showed that velocity profiles and reattachment lengths were predicted reasonably well by all three methods, while the skin friction coefficients were more difficult to predict accurately. It was noted that in general, selecting an appropriate solver for each problem to be considered is important.

INTRODUCTION

In the application of computational fluid dynamic (CFD) methods, some considerations are the relative accuracy, efficiency, and applicability of different flow solvers. Selecting an appropriate solver for a given problem based on those criteria is an important factor in the successful use of CFD. Conversely, selecting an inappropriate solver can result in an inaccurate solution, a waste of computer resources, excessive user effort, a solution with insufficient detail, a solution with overwhelming detail, or a failure to obtain any solution at all.

Validation is a first step in applying CFD to any problem. This is accomplished by running the solver on appropriate benchmark cases and comparing the solutions with experimental results, or better yet, by identifying such validation cases that have already been performed. The benchmark cases, which can vary in complexity and size, should encompass the main fluid dynamic features contained in the problem to be investigated.

For air breathing propulsion systems, separated-reattaching flows are of interest, especially as they apply to areas such as diffusers and nozzle boattails, because the presence and characteristics of separated-reattaching flow on these components can drastically alter their performance. In these flows, the separation is driven by boundary layer development and pressure gradients in the flow over a complex geometry, so predicting the separation point is a difficult task.

A classic benchmark case used for validating CFD codes for turbulent separated-reattaching flows is the flow over a backward-facing step (BFS). The geometry of the configuration is simple, but the flow is still complex and challenging to simulate, involving flow physics such as free shear layers, reattaching flow, and recirculation. Proper modeling of turbulence is needed for accurate simulation of the flow, and many studies applying different turbulence models to BFS flows have been conducted, such as in references 1-3. In BFS flow,

the separation point is fixed at the corner of the step; the separation is not driven by boundary layer development and adverse pressure gradients. Thus the problem is simplified considerably, facilitating study of the reattachment itself.

In order to assess the application of different CFD solvers to separated-reattaching flows, a comparative study was conducted for solutions to flow over BFS. Three Reynolds-averaged Navier-Stokes flow solvers incorporating two-equation k-ε turbulence models were used, each one using a different solution algorithm: a finite difference method (FDM) solver originally oriented to aeropropulsion flows, a computer aided engineering (CAE) oriented finite element method (FEM) code, and a CAE oriented hybrid finite element - finite difference method (HM) solver. FDM used a low Reynolds number k-ε turbulence (LR k-ε) model, whereas FEM and HM used versions of high Reynolds number k-ε turbulence (HR k-ε) models. Solutions were compared with each other, and with existing experimental data. This is not a comparison between numerical algorithms of finite differences and finite elements, due to a number of factors, and particularly because of differences in the turbulence models used.

EXPERIMENTAL STUDY

The experimental study of flow over BFS conducted by Driver and Seegmiller (4) was selected for use in the present work, because of the extensive quantitative measurements made, the relatively high flow speeds, and the low streamwise pressure gradient of the flow. The freestream velocity was 145 ft/s (Mach number = 0.128) in standard atmosphere, and the step height was 0.5 inches, giving a step height Reynolds number of 33420. The Reynolds number of the boundary layer momentum thickness 4 step heights upstream of the step was 5000, producing a fully turbulent boundary layer. The ratio of step height to tunnel exit height was 1:9 for the parallel wall case, so the streamwise pressure gradient due to the step was relatively small. Mean and turbulent flow velocity components were obtained using two component laser doppler velocimetry (LDV), wall static pressures downstream of the step were measured by static taps, and wall friction coefficients were obtained from oil-flow laser interferometry. Turbulence intensities, correlations, and dissipation were computed from LDV data.

COMPUTATIONAL METHODS

Three Reynolds-averaged Navier-Stokes flow solvers with k-ε turbulence models were used to solve BFS flow, each using a different solution algorithm: FDM with LR k-ε, FEM with HR k-ε, and HM with HR k-ε. HR k-ε assumes law-of-the-wall profiles in the boundary layer, whereas LR k-ε requires a large number (20+) of grid points near the wall to numerically resolve the boundary layer. Therefore, although LR k-ε is much more computationally intensive than HR k-ε, LR k-ε is usually expected to be more accurate for separated flows, because it does not assume the law-of-the-wall profiles that are based on attached flat plate boundary layers. The computational domain, schematically depicted in figure 1, begins four step heights upstream of the step where an incoming boundary layer velocity profile is specified, and ends far downstream of the step. HM and FEM use the same grid; FDM uses a much finer grid in order to accommodate the LR k-ε model.

Finite Difference Method (FDM)

The finite difference solver used in this study is PARC, an internal flow Navier-Stokes code used extensively by government and industry to analyze propulsion flows (5,6). Two-

dimensional / axisymmetric (2D), and three-dimensional (3D) versions are available. PARC was derived from the ARC Navier-Stokes code (7) which has been used for external flow calculations.

The governing equations of motion are the time dependent Reynolds averaged Navier-Stokes equations using a perfect gas relationship and Fourier's heat conduction law. These equations are discretized in conservation law form with respect to general curvilinear coordinates and solved with the Beam and Warming approximate factorization algorithm (8). Although the time dependent formulation of the equations is used, the code is intended for steady state flow simulations. The LR k-ε model of Chien (9), including modifications for compressibility by Nichols (10), was used in these calculations using the 2D version of the code.

A 11,341 point grid was used, with 111 points in the horizontal direction and 131 points in the vertical direction downstream of the step. In the boundary layers, the grid was packed to the walls such that downstream of the reattachment point, on the average, the first grid point off the wall was approximately at $y+ \sim 1.0$.

Finite Element Method (FEM)

The finite element solver used is FIDAP Version 5.04 by Fluid Dynamics International (11). It is intended to handle a wide variety of applications, including: internal and external aerodynamics, heat transfer, crystal growth, extrusion, injection molding, chemical mixing, chemical vapor deposition, etc. The code includes its own pre and post-processors to form a complete, integrated analysis package. Files can also be imported from, or exported to, other finite element pre/post-processors such as PATRAN, ANSYS, and SUPERTAB.

FEM uses the incompressible, Reynolds-averaged Navier-Stokes equations in either dimensional or non-dimensional form. Non-inertial frames of reference are supported, as are free surfaces. The Galerkin method of weighted residuals is used for finite-element formulation of the problem. A streamline upwinding capability is included to handle the numerical instabilities posed by Galerkin's method. Also, the standard pressure discretization can be replaced by a penalty function approximation. Several methods are available for solving the discrete system of equations including successive substitution, Newton-Raphson, and modified Newton-Raphson methods.

The HR k-ε model of Launder and Spalding (12), generally considered the 'standard' HR k-ε model, is used. However the treatment at the wall differs from that used in the HM (to be discussed later). In order to solve the full set of elliptic equations down through the viscous sublayer to the wall, a one-element thick layer of special wall elements are used adjacent to the physical boundary. These wall elements specify shape functions based on the law-of-the-wall profiles to characterize the variations in the mean flow variables. Then, van Driest's mixing length approach is used to model the variations of turbulent quantities. Alternatively, a user-defined algebraic turbulence model (based on mixing-length theory) could be created and used in place of HR k-ε; however, this option was not exercised in the present study.

The computational grid was generated using the mesh generator integrated with the FEM system. With the exception of the additional wall elements, the grid is identical to the one used with HM, consisting of 2751 nodes and 2796 elements, with 70 elements in the horizontal direction, and 40 elements in the vertical direction downstream of the step.

Hybrid Method (HM)

FLOTRAN version 2.0, by Compuflo, Inc. (13) uses a hybrid finite-element / finite-difference method. The solution algorithm is based on finite element methods. However, certain modifications make the computational efficiency and storage requirements more competitive with finite difference / finite volume codes, while still retaining the geometric flexibility of finite

element codes. This program consists of the flow solver only; grid generation and post processing are handled by finite element pre/post processors, such as PATRAN, ANSYS and I-DEAS.

The governing equations are the steady, Reynolds averaged Navier-Stokes equations, used in the incompressible form for the present problem. Galerkin's method of weighted residuals is used to discretize the diffusion and source terms. A monotone streamline upwind method is used to discretize the advection terms, in order to avoid oscillations in the advection terms, called dispersion errors, caused by the Galerkin's method. The intent of streamwise upwinding is to minimize the 'crosswind' numerical diffusion that may occur when the fluid flows diagonally across the cell. Pressure is derived from a velocity-pressure relation.

As in FEM, the Launder and Spalding HR k-ε turbulence model is used (11). Analytical law of the wall and log law of the wall velocity profiles are used, but the exact treatment near the wall differs from that used in FEM.

The grid used by HM in the present study was generated using PATRAN. In order to check the grid sensitivity, two grids were created: a coarse grid with 2640 elements, and a fine grid with about 6000 elements. However, both produced nearly identical solutions, therefore results shown herein are with the coarse grid, which is nearly identical to the grid used by FEM.

RESULTS

Reattachment Length

A sensitive parameter often used to quantify the accuracy of solutions to BFS flow is the reattachment length, defined as the distance downstream of the step where the flow separating at the step corner reattaches with the bottom wall. Reattachment occurs where the velocity gradient off the wall is zero, or in other words, where the wall shear stress is zero. However, there appears to be an inconsistency in the experimental results (4). Driver and Seegmiller report a reattachment length of $x/H = 6.25$, as measured by laser interferometry. On the other hand, velocity profiles measured by LDV indicate a reattachment point just downstream of $x/H = 5$, and the profile at $x/H=6$ appears clearly attached. Driver & Seegmiller speculate the discrepancy may be due to a long, thin separated region along the wall with very small length scales; but no such flow was indicated even in FDM results using LR k-ε (which is expected to better resolve near-wall flows than HR k-ε). Based on the reattachment length determined from oil-flow interferometry, FDM gives a good prediction, whereas FEM and HM underpredict by about 12% and 17%, respectively (table 1). However, if one were to consider the reattachment length inferred by the LDV velocity profiles, FEM and HM give the better predictions.

Wall Shear Stresses

Present results concur with studies in the literature (1-3) that wall shear stresses downstream of the step are difficult to predict accurately, yet in general, accurate prediction of skin friction is important for calculating the drag of practical configurations. Figure 2 depicts the present results. FDM created significant under and over shoots of skin friction coefficients, behind and ahead of the reattachment point, respectively. FEM produced a reasonable looking curve, but it was slightly shifted to the left due to a short reattachment length. HM underpredicted the skin friction, and the curve was also shifted to the left due to a short reattachment length. Neither FEM nor HM appeared to reproduce the secondary recirculation zone near the base of the step, indicated experimentally by positive C_f values in that region.

Mean Velocity Profiles

Axial velocity profiles were predicted reasonably well by all three methods, at the stations x/H = 3, 6 and 12 downstream of the step (fig. 3). At x/H = 3, all three solutions look qualitatively similar, with the 'corner' in the velocity profile at the correct y height. At x/H = 6 and x/H = 12, the velocity profile corners are still at the correct heights, but all three methods slightly underpredict the velocity near the wall, with FDM having the greatest discrepancy, and HM the least.

DISCUSSION

Turbulence is a major phenomena in BFS flow, and as expected, turbulence models have been observed to significantly impact the CFD solutions. Because the turbulence models used in FDM, FEM and HM are not exactly the same, differences in the solutions are likely due at least in part to different turbulence models. Using LR k-ε, Avva, et al. (1) observed strong sensitivity of the skin friction results to grid refinement in the inner layer, by varying the number of grid points in the inner layer between 5 and 30. In the present study, for FDM with LR k-ε, approximately 18 grid points were in the inner layer, so the skin friction results may change with changes in the boundary layer grid. Conventional wisdom holds that HR k-ε is not accurate for separated flow, because it assumes an attached velocity profile at the wall. Failure of solvers equipped with HR k-ε (FEM and HM) to reproduce the secondary recirculation zone at the base of the step seems to support this assertion. However, when the overall situation is considered, the present study concurs with Avva, et al. (1) and Steffen (3) that high Re k-ε may actually be preferable to LR k-ε for some cases such as BFS flow, because HR k-ε uses less computer resources, is less grid-resolution sensitive, and produces results of similar quality overall, when compared to LR k-ε.

Computational efficiency is a consideration, since these codes may be applied to large, complex problems; to this end, simple benchmark cases should not consume large quantities of computer resources. To obtain the present solutions, FDM used 50,000 Cray Y-MP CPU seconds, FEM consumed 615 Y-MP CPU seconds, and HM used 2000 seconds on a VAX9000. FEM and HM appear to be substantially more CPU efficient than FDM, but some other factors need to be considered. This particular FDM code is known to be very slow to converge for low speed flows (freestream Mach number < 0.2). Convergence is much faster for higher Mach numbers that are more typical of aerospace applications. Furthermore, as discussed above, LR k-ε, used in FDM, is inherently more computer intensive than HR k-ε, used in FEM and HM. Therefore, if the problem under consideration has higher freestream velocities as is more typical of aerospace applications, or if a HR k-ε model is successfully integrated with FDM, the relative computational efficiency of FDM should improve substantially.

The present study is only one test case, with a single fixed flow regime and a certain set of flow features; to draw generalized conclusions regarding the merit or performance of the three codes based on this one case only would be misleading. The original objective of this work--which was not fully realized due to time and code capability constraints--was to investigate a number of geometrically simple benchmark cases encompassing most of the flow regimes and flow physics encountered in air breathing propulsion inlet and nozzle flows, using a number of different flow solvers. Compressible and supersonic flows are aspects of those flows, therefore a simple low angle 'bent wall' was selected as a benchmark case to evaluate solver performance at high subsonic and supersonic Mach numbers. However, the FEM version available at the time did not handle compressible or supersonic flow, and attempts to run this case on HM were unsuccessful. Therefore, it becomes clear that an appropriate flow solver must be chosen for each problem to be investigated, and that there is no one code that is ideal for solving all types of flow.

The U.S. Government does not endorse any commercially available program with respect to any other program.

ANSYS is a registered trademark of Swanson Analysis Systems, Inc.

FIDAP is a registered trademark of Fluid Dynamics International, Inc.

FLOTRAN is a registered trademark of Compuflo, Inc.

I-DEAS and SUPERTAB are registered trademarks of Structural Dynamics Research Corp.

PATRAN is a registered trademark of PDA Engineering.

REFERENCES

1. Avva, R., Smith, C. and Singhal, A., "Comparative Study of High and Low Reynolds Number Versions of k-e Models," AIAA Paper 90-0246, 1990.
2. Georgiadis, N. J., Drummond, J. E., and Leonard, B. P., "Development of an Algebraic Turbulence Model for Analysis of Propulsion Flows," AIAA Paper 92-3861 or NASA TM-105701, 1992.
3. Steffen, C. J. Jr., "A Critical Comparison of Several Low Reynolds Number k-ε Turbulence Models for Flow Over a Backward-Facing Step", NASA TM to be published, 1993.
4. Driver, D. M. and Seegmiller, H. L., "Features of a Reattaching Turbulent Shear Layer in Divergent Channel Flow," *AIAA Journal*, Vol. 24, No. 2, 1985, pp. 163-171.
5. Cooper, G. K. and Sirbaugh, J. R., "PARC Code: Theory and Usage," AEDC-TR-89-15, 1989.
6. Cooper, G.K. and Sirbaugh, J.R., "The PARC Distinction: A Practical Flow Simulator," AIAA Paper 90-2002, 1990.
7. Pulliam, T.H., "Euler and Thin Layer Navier-Stokes Codes: ARC2D, ARC3D," Notes for Computational Fluid Dynamics User's Workshop, The University of Tennessee Space Institute, Tullahoma, Tennessee, (UTSI Publication E02-4005-023-84), 1984, pp. 15.1-15.85.
8. Beam, R.M., and Warming, R.F., "An Implicit Finite-Difference Algorithm for Hyperbolic Systems in Conservation-Law Form–Application to Eulerian Gasdynamic Equations," *Journal of Computational Physics*, Vol. 22, No. 1, 1976, pp. 87-110.
9. Chien, K.-Y., "Predictions of Channel and Boundary-Layer Flows with a Low-Reynolds-Number Turbulence Model," *AIAA Journal*, Vol. 20, No. 1, 1982, pp. 33-38.
10. Nichols, R.H., "A Two-Equation Model for Compressible Flows," AIAA Paper 90-0494, 1990.
11. *FIDAP Theoretical Manual: Revision 5.0*, Fluid Dynamics International, Inc., Evanston, IL, 1990.
12. Launder, B. E., and Spalding, D. B., "The Numerical Computation of Turbulent Flows," *Comp. Methods in Appl. Mech Engr.*, Vol. 3, 1974, pp. 269-289.
13. *FLOTRAN Theoretical Manual*, Compuflo, Inc. Charlottesville, VA., 1992.

Table 1. Reattachment lengths

Method	reattachment length (x/H)
Driver-Seegmiller Data	6.25
FDM	6.26
FEM	5.47
HM	5.22

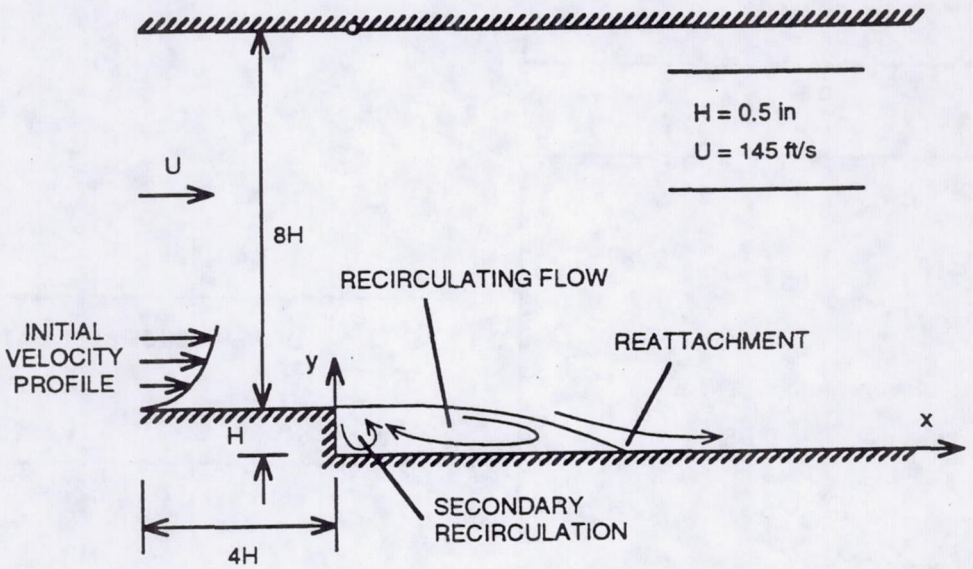

Figure 1. Schematic diagram of backward-facing step

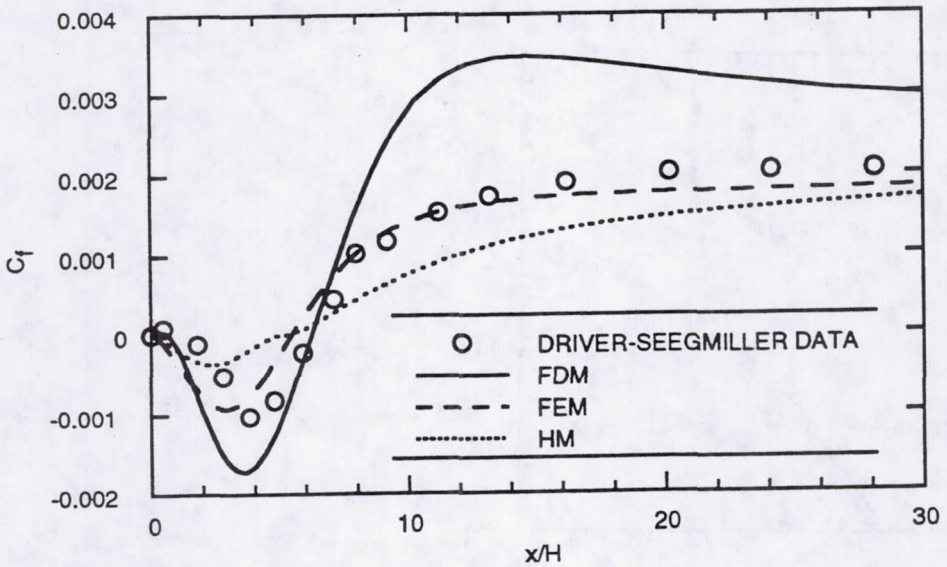

Figure 2. Wall skin friction coefficient distributions

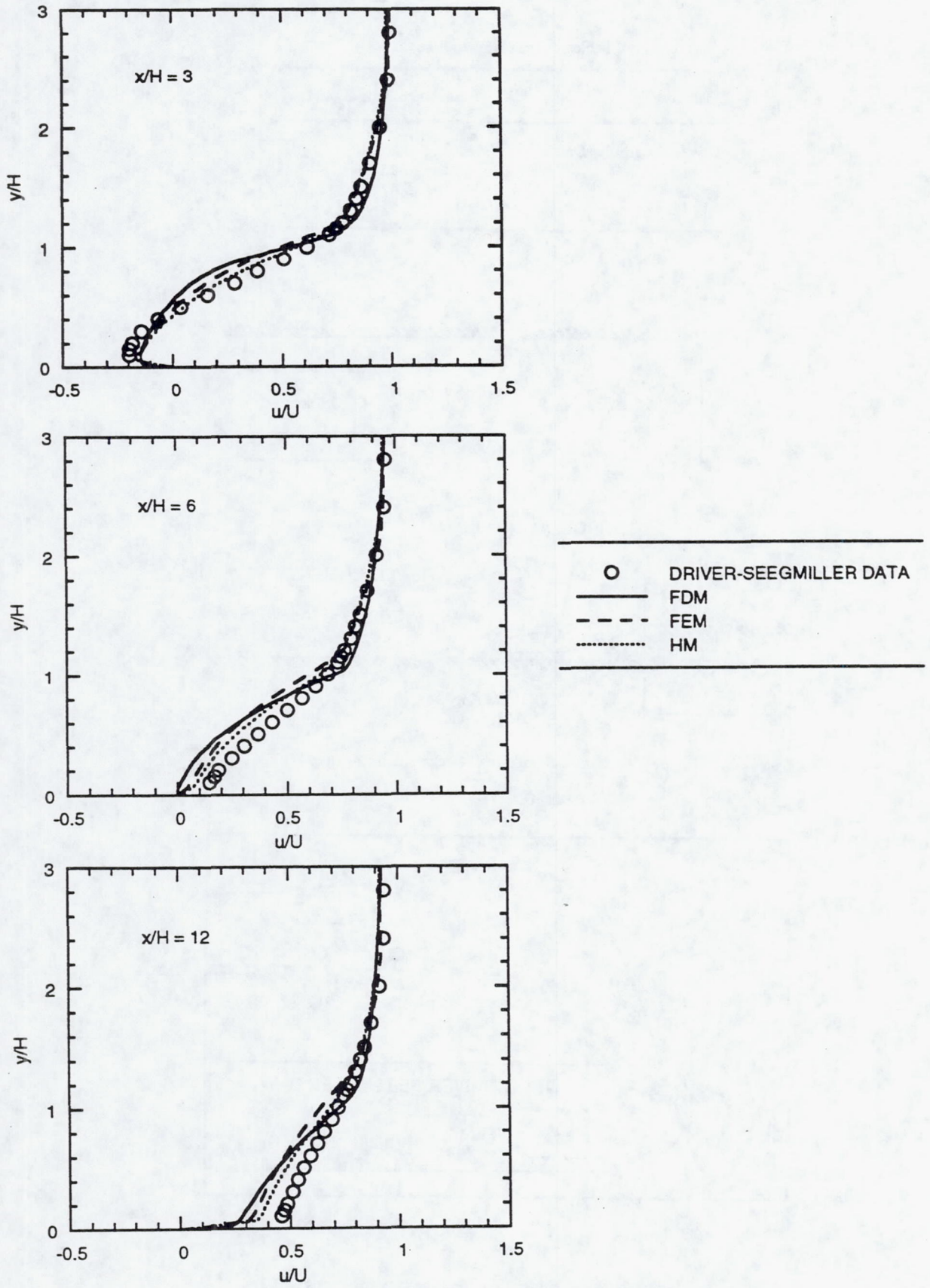

Figure 3. Mean velocity profiles in the separated and reattached regions